Frequency discontinuity and amplitude death with time-delay asymmetry

Nirmal Punetha,[1] Rajat Karnatak,[1,*] Awadhesh Prasad,[2,3] Jürgen Kurths,[4] and Ram Ramaswamy[1,5]
[1]*School of Physical Sciences, Jawaharlal Nehru University, New Delhi 110067, India*
[2]*Department of Physics and Astrophysics, University of Delhi, Delhi 110007, India*
[3]*MPI-PKS, Nöthnitzer Strasse 38, 01187 Dresden, Germany*
[4]*Potsdam Institute for Climate Impact Research, P.O. Box 601203, 14412 Potsdam, Germany*
[5]*University of Hyderabad, Hyderabad 500 046, India*
(Received 16 November 2011; revised manuscript received 13 February 2012; published 5 April 2012)

We consider oscillators coupled with asymmetric time delays, namely, when the speed of information transfer is direction dependent. As the coupling parameter is varied, there is a regime of amplitude death within which there is a phase-flip transition. At this transition the frequency changes discontinuously, but unlike the equal delay case when the relative phase difference changes by π, here the phase difference changes by an arbitrary value that depends on the difference in delays. We consider asymmetric delays in coupled Landau-Stuart oscillators and Rössler oscillators. Analytical estimates of phase synchronization frequencies and phase differences are obtained by separating the evolution equations into phase and amplitude components. Eigenvalues and eigenvectors of the Jacobian matrix in the neighborhood of the transition also show an "avoided crossing," as has been observed in previous studies with symmetric delays.

DOI: 10.1103/PhysRevE.85.046204 PACS number(s): 05.45.Ac, 05.45.Pq, 05.45.Xt

I. INTRODUCTION

A subject of continuing interest in the study of nonlinear dynamical systems is the nature of dynamics that results when two or more such systems are coupled. Such coupling is typically mediated through signals that are transmitted from one system to another, and in most natural systems, such signals travel with a finite speed. Models of coupled systems therefore frequently account for this feature through time-delay coupling, and this has been extensively studied in a wide variety of systems in physics, biology, ecology, and sociology [1–3]. A large number of studies have examined the consequences of different forms of coupling; these include synchronization, phase locking, phase drift, phase flip, hysteresis, amplitude death, etc. [4–7].

When signals are transmitted in the presence of an external field, there can be an additional effect of directionality: the time delays in both directions need not be identical. If τ_{ij} is the time delay for a signal to go from system j to system i, we examine here the situation when $\tau_{ij} \neq \tau_{ji}$, and in particular, how this asymmetry affects phenomena that are known to occur when the time delay is symmetric ($\tau_{ij} = \tau_{ji}$). Note that if both delays are equal to 0, this reduces to instantaneous coupling, while if one of the $\tau's \to \infty$, this means that the signal does not reach the other system in finite time and hence the coupling effectively becomes unidirectional [8].

A phenomenon that frequently arises in time-delay coupled systems is amplitude death (AD) [9–18]. A number of studies have extensively investigated the origins of AD through both numerical and analytic approaches, albeit with symmetric delays. Associated with AD, although not restricted to it, is a transition that occurs in coupled systems: the phase flip [19,20], where the relative phases of the two synchronized subsystems undergo an abrupt change of π and the frequencies of oscillation also exhibit a discontinuous change [20,21]. Our concern in the present work is to study how these phenomena are affected with time-delay asymmetry, particulary in the AD regime where analytical study is possible.

We analyze coupled systems with varying and asymmetric time delays and observe that there can be an abrupt change in phase for specific values of the delays, but the difference takes a value that is not necessarily equal to π, as happens when the delays are identical. This phase discontinuity arises as a result of an abrupt change in the oscillation frequencies. For some purposes, a system with asymmetric delays can be shown to be effectively equivalent to a system where the delays are identical.

In Sec. II, we present results and analysis for coupled Landau-Stuart oscillators. Estimates for frequency and phase of the system are shown, and a comparison with the case of symmetric delays is presented. A detailed study of the eigenvalues and eigenvectors of the system in the vicinity of the transition is also presented. In Sec. III, coupled Rössler system is studied to generalize the study of asymmetric delays for chaotic systems. The results are summarized in Sec. IV.

II. COUPLED LANDAU-STUART OSCILLATORS

The Landau-Stuart (LS) oscillator is a well-studied periodic system, described as

$$\frac{dZ}{dt} = (A + \iota\omega - |Z|^2)Z. \tag{1}$$

The LS oscillator shows limit cycle motion near a Hopf bifurcation, with amplitude of oscillations being directly proportional to $\sqrt{A}$. Here ω is the intrinsic frequency of the oscillations, and $Z(t)$ is a complex variable. The dynamical equations for the asymmetric delay coupled oscillators can be

*Present address: ICBM, University of Oldenburg, 26111 Oldenburg, Germany.

 ©2012 American Physical Society

written as

$$\dot{Z}_1 = (A_1 + i\omega_1 - |Z_1|^2)Z_1 + K(Z_2(t-\tau_{12}) - Z_1),$$
$$\dot{Z}_2 = (A_2 + i\omega_2 - |Z_2|^2)Z_2 + K(Z_1(t-\tau_{21}) - Z_2). \quad (2)$$

We consider a case where $A_1 = A_2 = 1$, and for notational simplicity set $\tau_{ij} \equiv \tau_i$. In Cartesian coordinates, using $Z_j = x_j + iy_j$, the equations become

$$\dot{x}_i = (1 - |Z_i|^2)x_i - \omega_1 y_i + K[x_j(t-\tau_i) - x_i(t)]$$
$$\dot{y}_i = (1 - |Z_i|^2)y_i + \omega_2 x_i + K[y_j(t-\tau_i) - y_i(t)], \quad (3)$$

where $Z_i = \sqrt{x_i^2 + y_i^2}$, the indices $i, j = 1,2$, and the interaction strength is given by K. Introducing the phase and the amplitude variables

$$\Phi_i = \arctan(y_i/x_i) \quad R_i = \sqrt{x_i^2 + y_i^2}$$

and transforming Eq. (3) into polar coordinates, we get

$$\dot{R}_i = R_i\left(1 - K - R_i^2\right) + K R_j(t-\tau_i)\cos[\Phi_j(t-\tau_i) - \Phi_i],$$
$$\dot{\Phi}_i = \omega_i + K[R_j(t-\tau_i)/R_i]\sin[\Phi_j(t-\tau_i) - \Phi_i]. \quad (4)$$

If the amplitudes are constant, namely, $R_i(t-\tau)/R_j(t) = k_{i,j}$, then the equations for the phases simplify to

$$\dot{\Phi}_1 = \omega_1 + k_{1,2}K\sin(\Phi_2(t-\tau_1) - \Phi_1),$$
$$\dot{\Phi}_2 = \omega_2 + k_{2,1}K\sin(\Phi_1(t-\tau_2) - \Phi_2). \quad (5)$$

Equation (5) effectively models phase oscillators with asymmetry in coupling strengths (introduced by ratios $k_{i,j}$) and the time delays. For identical or nearly identical oscillators, we can consider $k_{i,j} = k_{j,i} \approx 1$, which gives

$$\dot{\Phi}_1 = \omega_1 + K\sin[\Phi_2(t-\tau_1) - \Phi_1]$$
$$\dot{\Phi}_2 = \omega_2 + K\sin[\Phi_1(t-\tau_2) - \Phi_2]. \quad (6)$$

Following Schuster and Wagner [3], we make the ansatz $\Phi_{1,2}(t) = \Omega t \pm \Delta\Phi/2$ for phase-synchronized (PS) solutions, where Ω is the common frequency and $\Delta\Phi$ is the phase difference between the oscillators. Substituting these in Eq. (6) and adding up the resultant equations, we get the following transcendental equation for the collective frequency:

$$\Omega = \bar{\omega} - K\sin(\Omega\bar{\tau})\cos\left(\frac{\Omega\Delta\tau}{2} + \Delta\Phi\right). \quad (7)$$

Similarly, the difference in Eqs. (6) gives

$$\sin\left(\frac{\Omega\Delta\tau}{2} + \Delta\Phi\right) = \frac{\Delta\omega}{2K\cos(\Omega\bar{\tau})}, \quad (8)$$

where $\Delta\tau = (\tau_1 - \tau_2)$, $\bar{\tau} = (\tau_1 + \tau_2)/2$, $\Delta\omega = (\omega_1 - \omega_2)$, and $\bar{\omega} = (\omega_1 + \omega_2)/2$ for identical oscillators ($\omega_1 = \omega_2 = \omega$), which gives $\sin(\frac{\Omega\Delta\tau}{2} + \Delta\Phi) = 0 \Rightarrow \cos(\frac{\Omega\Delta\tau}{2} + \Delta\Phi) = \pm 1$. Therefore, using this, the transcendental Eq. (7) reduces to

$$\Omega = \omega \mp K\sin(\Omega\bar{\tau}). \quad (9)$$

The phase synchronous solutions satisfy Eq. (9) and consequently, the roots of equation

$$F_{\mp}(\Omega) = \omega - \Omega \mp K\sin(\Omega\bar{\tau}) \quad (10)$$

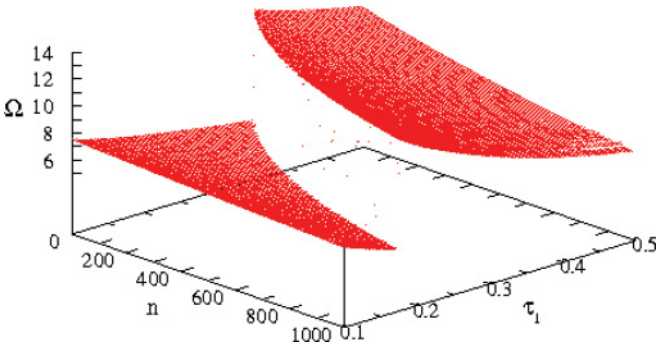

FIG. 1. (Color online) The variation of the common frequency Ω as a function of τ_1 and τ_2. $\tau_2 = (n/N)\tau_1$, where $N = 1000$ is the discretization taken in the simulation.

give the PS frequencies. The phase difference, from Eq. (8), is

$$\Delta\Phi = -\frac{\Omega\Delta\tau}{2} \quad \text{if} \quad \cos\Omega\bar{\tau} > 0$$
$$= \pi - \frac{\Omega\Delta\tau}{2} \quad \text{otherwise.} \quad (11)$$

Specifically for the case when $\tau_2 \leqslant \tau_1$, this reduces to

$$\Delta\Phi = \frac{\Omega|\Delta\tau|}{2} \quad \text{if} \quad \cos\Omega\bar{\tau} > 0$$
$$= \pi + \frac{\Omega|\Delta\tau|}{2} \quad \text{otherwise.} \quad (12)$$

The roots of the transcendental equation Eq. (10) give the allowed PS frequency solutions (Ω).

Shown in Figs. 1 and 2 are the common frequency and the phase difference ($\Delta\Phi = \Phi_1 - \Phi_2$), calculated numerically [22] from Eq. (3), as a function of τ_1 and τ_2. A line of phase difference discontinuity as well as the frequency jump [19] can be seen in the diagrams. The parameter values for the numerics are $\omega_1 = \omega_2 = 9$ and $K = 5$. The numerical results of the original system, namely, Eq. (3), are compared with the analytic results for the frequencies in Fig. 3(a) at a particular value of $n = 500$. Equation (11) gives an analytical estimate of the phase difference $\Delta\Phi$, which depends on the difference between the delay times: in general, it is neither zero nor π, as can be seen in Fig. 3(b).

The dependence of Ω on the arithmetic mean of the asymmetric delays $\bar{\tau} = (\tau_1 + \tau_2)/2$ has the interesting consequence

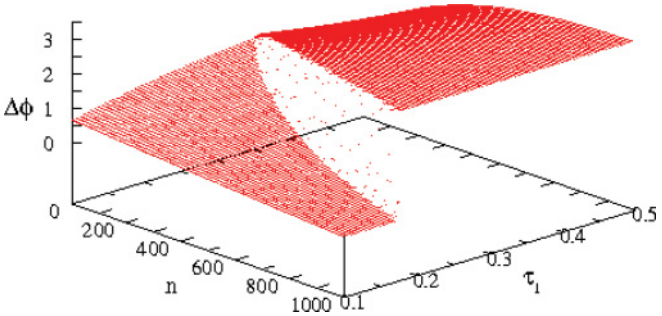

FIG. 2. (Color online) The variation of the phase difference as a function of τ_1 and τ_2. n and N are the same as in Fig. 1.

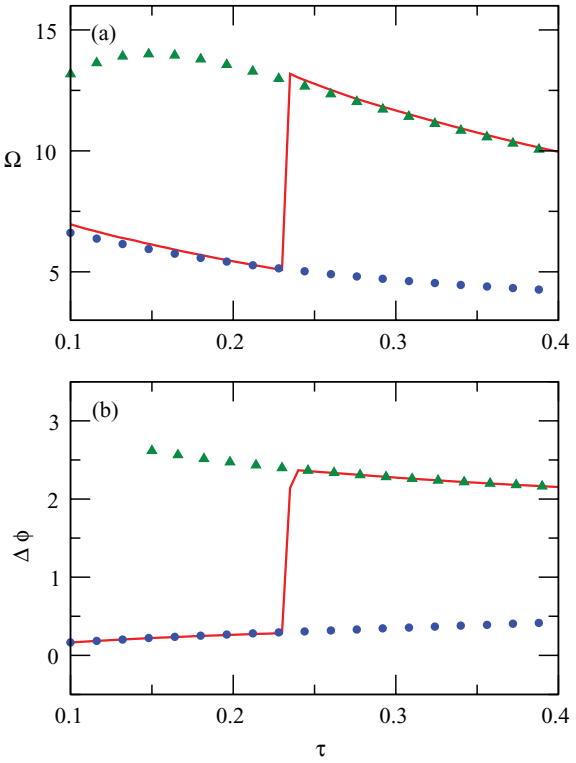

FIG. 3. (Color online) (a) Synchronized frequency Ω and (b) phase difference $\Delta\Phi$ for the Landau-Stuart system with $\tau_1 = \tau$ and $\tau_2 = \tau/2$. The solid lines are the numerical results from the model [Eq. (3)], while the circles and triangles in (a) and (b) correspond to analytical estimation from Eqs. (10) and (11), respectively.

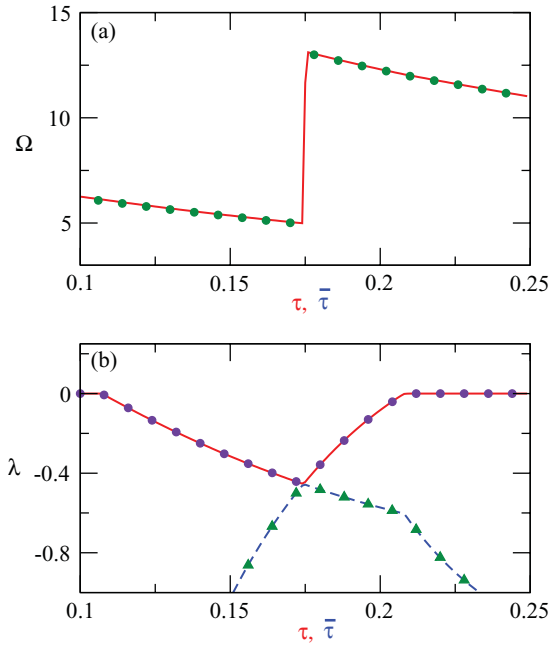

FIG. 4. (Color online) Variation of (a) frequency and (b) Lyapunov exponents for the Landau-Stuart system as function of symmetric delay τ (solid red line in the upper portion and dashed blue line in the lower portion of the figure) and asymmetric delays, $\tau_1 = 0$ and $\tau_2 = 2\tau$ (circles and triangles), so that the average delay $\bar{\tau}$ is the same.

that for a system with the same average delay, the frequency response is identical [see Fig. 4(a)]. In order to understand this consequence, we next analyze this transition in terms of the eigenvalues and eigenvectors of the Jacobian matrix at the fixed point [21]. For the Landau-Stuart system, the origin is the stable fixed point in the AD regime. The Jacobian matrix at the origin is

$$\mathbf{J} = \begin{pmatrix} A + \iota\omega - K & Ke^{-\lambda\tau_1} \\ Ke^{-\lambda\tau_2} & A + \iota\omega - K \end{pmatrix}. \tag{13}$$

The characteristic equation of the Jacobian $\mathbf{J} - \lambda\mathbf{I} = 0$ gives

$$(\lambda - A - \iota\omega + K)^2 - K^2 e^{-\lambda(\tau_1+\tau_2)} = 0. \tag{14}$$

Looking at the characteristic equation, we can conclude that the eigenvalues of the system in the AD regime are the functions of the arithmetic mean of the delays $\bar{\tau}$. This implies that the Lyapunov spectrum of the system for some fixed value of $\bar{\tau}$ is identical for the same fixed point (is independent of the values of τ_1 or τ_2 given the arithmetic mean stays fixed). For the Landau-Stuart system, this is shown in Fig. 4(b). Substituting $\lambda = \alpha + i\beta$ and $(\tau_1 + \tau_2) = 2\bar{\tau}$ for the complex eigenvalues in Eq. (14) and separating out the real and imaginary parts, we get

$$\alpha^2 - \beta^2 + 2\alpha(K - A) + K - A^2 + 2\beta\omega - \omega^2 - K^2 e^{-2\alpha\bar{\tau}} \cos(2\beta\bar{\tau}) = 0, \tag{15}$$

and

$$2\alpha(\beta - \omega) + 2(K - A)(\beta - \omega) + K^2 e^{-2\alpha\bar{\tau}} \sin(2\beta\bar{\tau}) = 0. \tag{16}$$

Solving these equations simultaneously, we find complex conjugate pairs $(\alpha_i \pm \iota\beta_i)$ as solutions and one obtains the real parts α's which correspond to the Lyapunov exponents and the corresponding imaginary parts β's in the AD regime. The β corresponding to the largest real part corresponds to the oscillation frequency for the system. These are shown (with symbols) along with the numerically determined quantities (solid and dashed lines) for the original system, namely, Eq. (3), in Fig. 5, which match well. We also see the "avoided crossing" [23] of the Lyapunov exponents [Fig. 5(a)]: since Lyapunov exponents are ordered by rank, they cannot in principle cross one other. At this avoided crossing, however, pairs of eigenvalues interchange their imaginary part [21]. Since the imaginary part of the largest eigenvalue corresponds to the oscillation frequency, there is a jump in the frequency at this transition as seen in Fig. 5(b), where the system moves from the lower frequency branch β_1 to the higher β_2. This transition is similar as in the previous work with symmetric delays [21]. Indeed, much of the analysis that can be carried out for the symmetric delay case [21] for the Lyapunov vectors associated with these eigenvalues carries over here. Defining the order parameter γ as a scalar product,

$$\gamma_k(\bar{\tau}) = \langle \mathbf{e_k}(\bar{\tau}')|\mathbf{e_k}(\bar{\tau})\rangle^2, \tag{17}$$

where k is the Lyapunov eigenvector index with $k = 1$ being the eigenvector corresponding to the largest Lyapunov

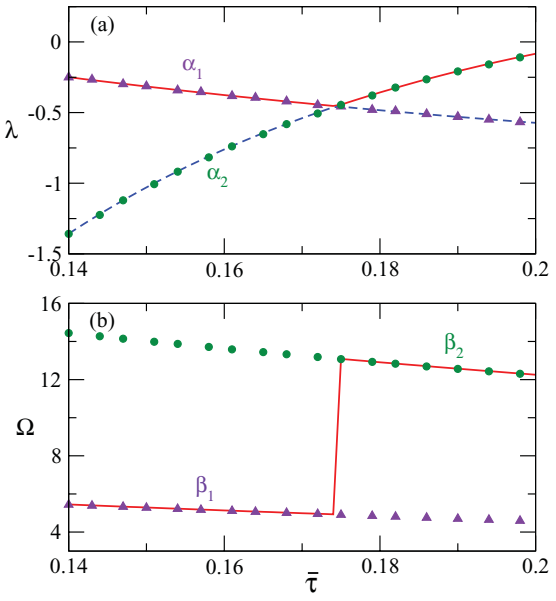

FIG. 5. (Color online) (a) Lyapunov exponents (solid red line in the upper portion and dashed blue line in the lower portion of the figure) and real part of the eigenvalues of the Jacobian (circles and triangles) for the coupled system in the AD region. (b) The common frequencies (solid line) and the imaginary part of the eigenvalues (circles and triangles) of the Jacobian [Eq. (13)].

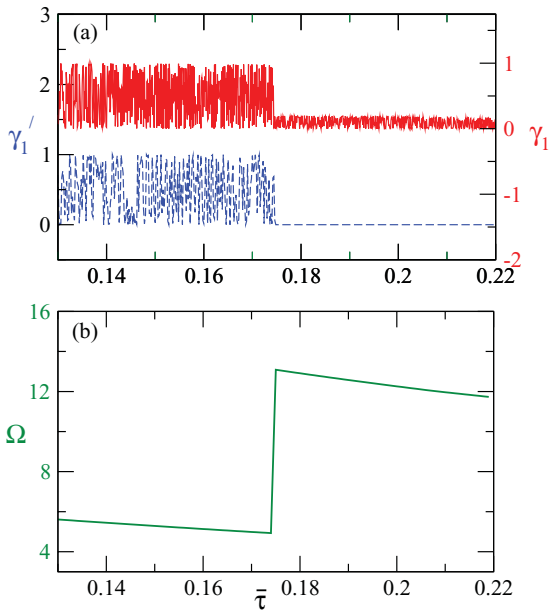

FIG. 6. (Color online) (a) Order parameter γ_1 showing the change in behavior of the eigenvectors at the delay value where the transition occurs. The blue dashed curve in the lower portion of the figure corresponds to the case of symmetric delays in the coupling, whereas the red solid curve (upper portion) is for the case with asymmetric delays: $\tau_1 = 0$ and $\tau_2 = 2\tau$. (b) Frequency Ω for the system with asymmetric time-delay coupling with $\tau_1 = 0$ and $\tau_2 = 2\tau$.

exponent, and $\bar{\tau}'$ is fixed at a particular value of the delay prior to the transition. The variation of γ_1 is shown in Fig. 6 along with the frequency jump. A change in the qualitative behavior of the order parameter is clearly seen before and after the transition point. The only difference from symmetric delays to asymmetry delay is that the order parameter γ_1 becomes zero after the transition for the former case [21] while it remains nonzero after the transition in the latter.

Based on the above results, we can safely conclude that the basic mechanism of phase flip proposed previously for the symmetric delays [21] holds in the case of asymmetric delays as well.

III. COUPLED RÖSSLER SYSTEM

In this section, we analyze coupled chaotic Rössler oscillators [24] with unequal delays in an attempt to generalize the results obtained in Sec. II for chaotic systems. The equations for the coupled Rössler oscillators can be written as

$$\begin{aligned} \dot{x_1} &= -\omega_1 y_1 - z_1 + \epsilon[x_2(t-\tau_1) - x_1(t)], \\ \dot{y_1} &= \omega_1 x_1 + a y_1, \quad \dot{z_1} = f + z_1(x_1 - c), \\ \dot{x_2} &= -\omega_2 y_2 - z_2 + \epsilon[x_1(t-\tau_2) - x_2(t)] \\ \dot{y_2} &= \omega_2 x_2 + a y_2, \quad \dot{z_2} = f + z_2(x_2 - c). \end{aligned} \tag{18}$$

For the numerics, we consider identical oscillators with the parameters $a = 0.165$, $f = 0.2$, $c = 10$, and $\omega_1 = \omega_2 = 0.99$ such that the motion of the individual oscillators is chaotic [25]. The numerically calculated synchronized frequency Ω and the phase differences ($\Delta\Phi = \Phi_1 - \Phi_2$) for different delays [Eq. (18)] at the coupling strength $\epsilon = 1.5$ are shown in Figs. 7 and 8, respectively. Since we consider the oscillators to be in the phase coherent regime, the phase and the amplitude can be defined by introducing the variables $\phi_i = \arctan(y_i/x_i)$ and $A_i = \sqrt{x_i^2 + y_i^2}$ [6]. Rewriting the system equations in terms of the phase and the amplitude gives

$$\begin{aligned} &\dot{A}_{1,2}\cos(\phi_{1,2}) - A_{1,2}\sin(\phi_{1,2})\dot{\phi}_{1,2} \\ &\quad = -\omega_{1,2}A_{1,2}\sin(\phi_{1,2}) - z_{1,2} + \epsilon\{A_2(t-\tau_{1,2}) \\ &\qquad \times \cos[\phi_{2,1}(t-\tau_{1,2})] - A_{1,2}\cos\phi_{1,2}\} \\ &\dot{A}_{1,2}\sin(\phi_{1,2}) + A_{1,2}\cos(\phi_{1,2})\dot{\phi}_{1,2} \\ &\quad = \omega_{1,2}A_{1,2}\cos(\phi_{1,2}) + aA_{1,2}\sin\phi_{1,2} \\ &\dot{z}_{1,2} = f + z_{1,2}(A_{1,2}\cos\phi_{1,2} - c). \end{aligned}$$

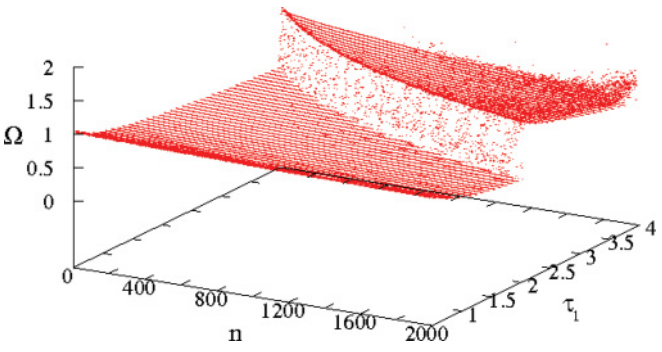

FIG. 7. (Color online) Variation of the common frequency Ω as a function of τ_1 and τ_2 similar to Fig. 1. $\tau_2 = (n/N)\tau_1$, and the discretization taken in the simulation $N = 2000$.

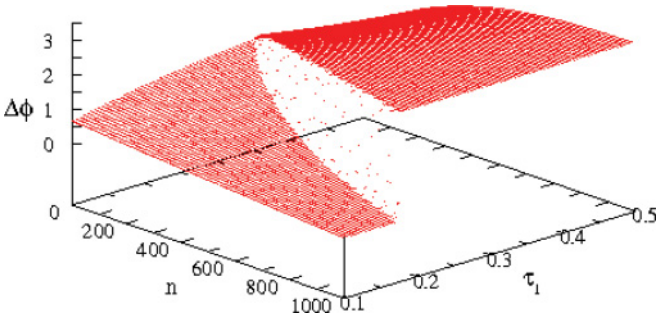

FIG. 8. (Color online) Variation of the phase difference as a function of τ_1 and τ_2. n and N are the same as in Fig. 7.

For each oscillator, solving the first two expressions to find the the values of $\dot{A}_{1,2}$ and $\dot{\phi}_{1,2}$ gives

$$\begin{aligned}
\dot{A_1} &= aA_1\sin^2\phi_1 - z_1\cos\phi_1 + \epsilon[A_2(t-\tau_1)\cos\phi_2(t-\tau_1)\\
&\quad\times\cos\phi_1 - A_1\cos^2\phi_1],\\
\dot{\phi_1} &= \omega_1 + a\sin\phi_1\cos\phi_1 + z_1\sin\phi_1/A_1 - \epsilon[A_2(t-\tau_1)\\
&\quad\times\cos\phi_2(t-\tau_1)\sin\phi_1/A_1 - \sin\phi_1\cos\phi_1],\\
\dot{z_1} &= f - cz_1 + A_1z_1\cos\phi_1,\\
\dot{A_2} &= aA_2\sin^2\phi_2 - z_2\cos\phi_2 + \epsilon[A_1(t-\tau_2)\cos\phi_1(t-\tau_2)\\
&\quad\times\cos\phi_2 - A_2\cos^2\phi_2],\\
\dot{\phi_2} &= \omega_2 + a\sin\phi_2\cos\phi_2 + z_2\sin\phi_2/A_2 - \epsilon[A_1(t-\tau_2),\\
&\quad\times\cos\phi_1(t-\tau_2)\sin\phi_2/A_2 - \sin\phi_2\cos\phi_2],\\
\dot{z_2} &= f - cz_2 + A_2z_2\cos\phi_2.
\end{aligned}$$

We analyze this system by averaging over the rotations of the phases $\phi_{1,2}$ [6,26]. Assuming that the amplitudes vary slowly, new "slow" phases θ can be introduced through the substitution $\phi_{1,2} = \omega_0 t + \theta_{1,2}$. Averaging the equations we get

$$\begin{aligned}
\omega_0 + \dot{\theta_1} &= \omega_1 + \epsilon\left(\frac{A_2(t-\tau_1)}{2A_1}\sin[\theta_2(t-\tau_1) - \theta_1 - \omega_0\tau_1]\right),\\
\omega_0 + \dot{\theta_2} &= \omega_2 + \epsilon\left(\frac{A_1(t-\tau_2)}{2A_2}\sin[\theta_1(t-\tau_2) - \theta_2 - \omega_0\tau_2]\right).
\end{aligned} \tag{19}$$

The substitution $\theta_{1,2}(t) = \Phi_{1,2}(t) - \omega_0 t$ transforms these equations to a corotating frame of ω_0, giving

$$\begin{aligned}
\dot{\Phi_1} &= \omega_1 + \epsilon\frac{A_2(t-\tau_1)}{2A_1}\sin[\Phi_2(t-\tau_1) - \Phi_1],\\
\dot{\Phi_2} &= \omega_2 + \epsilon\frac{A_1(t-\tau_2)}{2A_2}\sin[\Phi_1(t-\tau_2) - \Phi_2].
\end{aligned} \tag{20}$$

If the amplitudes are constant, namely, $A_{2,1}(t-\tau)/A_{1,2}(t) = k_{1,2}$, then the equations for the phases simplify to

$$\begin{aligned}
\dot{\Phi_1} &= \omega_1 + k_1\frac{\epsilon}{2}\sin[\Phi_2(t-\tau_1) - \Phi_1],\\
\dot{\Phi_2} &= \omega_2 + k_2\frac{\epsilon}{2}\sin[\Phi_1(t-\tau_2) - \Phi_2].
\end{aligned} \tag{21}$$

Equations (21) effectively model phase oscillators with asymmetry in coupling strengths (introduced by ratios $k_{1,2}$) and the time delays. For identical or nearly identical oscillators, we can consider $k_1 = k_2 \approx 1$, which gives

$$\begin{aligned}
\dot{\Phi_1} &= \omega_1 + K\sin[\Phi_2(t-\tau_1) - \Phi_1],\\
\dot{\Phi_2} &= \omega_2 + K\sin[\Phi_1(t-\tau_2) - \Phi_2],
\end{aligned} \tag{22}$$

where $K = \frac{\epsilon}{2}$. Equation (22) is the equation for two coupled phase oscillators with different delays and serves as a nice model to mimic the phase dynamics of the system in Eq. (18).

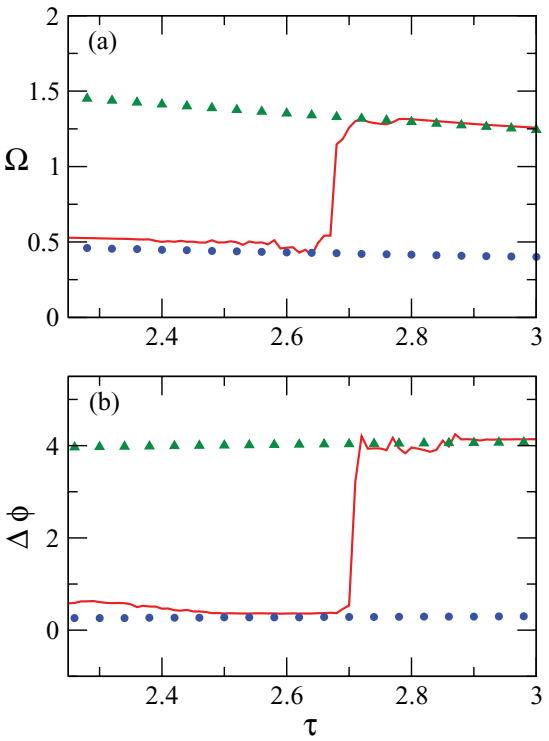

FIG. 9. (Color online) (a) Synchronized frequency Ω and (b) phase difference $\Delta\Phi$ for unequal delays $\tau_1 = \tau$ and $\tau_2 = \tau/2$. The solid lines are numerical results, while circles and triangles in (a) and (b) are the frequency and phase difference obtained analytically from Eq. (10) with effective coupling $K = \epsilon/2$ and Eq. (11), respectively.

We observe that the phase dynamics of the Rössler system is exactly identical to that of Eq. (6) with an effective coupling $K = \epsilon/2$. Following the procedure described before, we can obtain Eq. (10) for frequencies and Eq. (11) for the phase differences by substituting $K = \epsilon/2$. These analytical values, Ω and $\Delta\Phi$ (with symbols), are compared with the numerical quantities (with solid line) in Fig. 9. Note that while the agreement is fairly good, there is a small mismatch which can be ascribed to the approximations made in the derivation of Eq. (22). Since the frequency and phase estimates for the Rössler system are identical to the Landau-Stuart oscillators, this means that the frequency response is once again just dependent upon the average delay $\bar{\tau}$. This agreement between different delay and corresponding equivalent delay frequencies can be observed in Fig. 10(a).

Similar to the LS case, we next analyze the phase change transition in terms of the eigenvalues and eigenvectors of

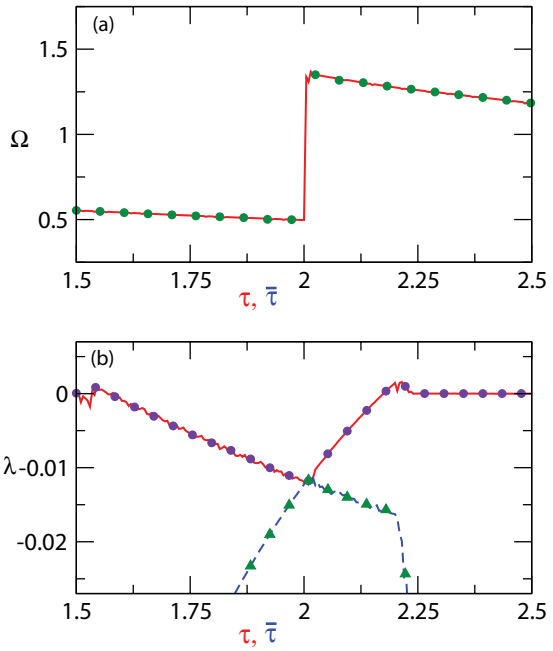

FIG. 10. (Color online) Variation of (a) frequency and (b) Lyapunov exponents for Rössler system as a function of symmetric delay τ (solid red line in the upper portion and dashed blue line in the lower portion of the figure) and asymmetric delays, $\tau_1 = 0$ and $\tau_2 = 2\tau$ (circles and triangles), so that the average delay $\bar{\tau}$ is the same.

the Jacobian matrix at the fixed point [27]. For the chaotic coupled Rössler systems, the fixed points are the roots of the equations

$$\begin{aligned} -\omega_1 y_1^* - z_1^* + \epsilon(x_2^* - x_1^*) &= 0, \\ \omega_1 x_1^* + a y_1^* &= 0, \\ f + z_1^*(x_1^* - c) &= 0, \\ -\omega_2 y_2^* - z_2^* + \epsilon(x_1^* - x_2^*) &= 0, \\ \omega_2 x_2^* + a y_2^* &= 0, \\ f + z_2^*(x_2^* - c) &= 0. \end{aligned} \tag{23}$$

The stable fixed point solutions in the AD regime are of the completely synchronous form $(x^*, y^*, z^*, x^*, y^*, z^*)$. These fixed point can be computed by solving the above equations and are given as

$$\begin{aligned} x_1^* = x_2^* &= \frac{1}{2\omega}(c\omega \pm \sqrt{c^2\omega^2 - 4af}), \\ y_1^* = y_2^* &= -\frac{1}{2a}(c\omega \pm \sqrt{c^2\omega^2 - 4af}), \\ z_1^* = z_2^* &= \frac{\omega}{2a}(c\omega \pm \sqrt{c^2\omega^2 - 4af}), \end{aligned} \tag{24}$$

and the stable fixed point solutions are [27]

$$\begin{aligned} x_1^* = x_2^* &= \frac{1}{2\omega}(c\omega - \sqrt{c^2\omega^2 - 4af}), \\ y_1^* = y_2^* &= -\frac{1}{2a}(c\omega - \sqrt{c^2\omega^2 - 4af}), \\ z_1^* = z_2^* &= \frac{\omega}{2a}(c\omega - \sqrt{c^2\omega^2 - 4af}). \end{aligned} \tag{25}$$

The Jacobian matrix for the coupled Rössler system at the fixed point can be written as

$$\mathbf{J} = \begin{pmatrix} -\epsilon & -\omega & -1 & \epsilon e^{-\lambda\tau_1} & 0 & 0 \\ \omega & a & 0 & 0 & 0 & 0 \\ z^* & 0 & (x^* - c) & 0 & 0 & 0 \\ \epsilon e^{-\lambda\tau_2} & 0 & 0 & -\epsilon & -\omega & -1 \\ 0 & 0 & 0 & \omega & a & 0 \\ 0 & 0 & 0 & z^* & 0 & (x^* - c) \end{pmatrix}. \tag{26}$$

The characteristic equation $(\mathbf{J} - \lambda\mathbf{I}) = 0$ is obtained as the polynomial [28]:

$$\begin{aligned} &[(-\epsilon - \lambda)(a - \lambda)(x^* - c - \lambda) + \omega^2(x^* - c - \lambda) \\ &\quad + z^*(a - \lambda)]^2 - \epsilon^2(e^{-\lambda(\tau_1+\tau_2)})a^2(x^* - c)^2 = 0. \end{aligned} \tag{27}$$

We substitute $\lambda = \alpha + i\beta$ and $(\tau_1 + \tau_2) = 2\bar{\tau}$ for the eigenvalues in Eq. (27) and separate out the real and imaginary parts of the equation. The expression for the real part is

$$\begin{aligned} &c_0 + c_1\alpha + c_2(\alpha^2 - \beta^2) + c_3(\alpha^3 - 3\alpha\beta^2) \\ &\quad + c_4(\alpha^4 + \beta^4 - 6\alpha^2\beta^2) + c_5(\alpha^5 + 5\alpha\beta^4 - 10\alpha^3\beta^2) \\ &\quad + c_6(\alpha^6 - \beta^6 + 15\alpha^2\beta^4 - 15\alpha^4\beta^2) + [b_0 + b_1\alpha \\ &\quad + b_2(\alpha^2 - \beta^2) + b_3(\alpha^3 - 3\alpha\beta^2) + b_4(\alpha^4 + \beta^4 - 6\alpha^2\beta^2)] \\ &\quad \times \cos(2\beta\bar{\tau})e^{-2\alpha\bar{\tau}} + [b_1\beta + b_2(2\alpha\beta) + b_3(3\alpha^2\beta - \beta^3) \\ &\quad + b_4(4\alpha^3\beta - 4\alpha\beta^3)]\sin(2\beta\bar{\tau})e^{-2\alpha\bar{\tau}} = 0, \end{aligned} \tag{28}$$

where the coefficients c_i's $(i = 0...6)$ and b_j's $(j = 0...4)$ are the functions of the fixed points, system parameters, and the coupling strength. Similarly for the imaginary part,

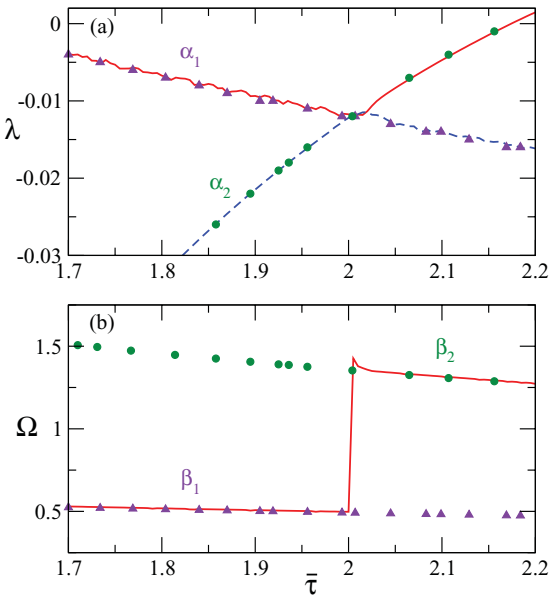

FIG. 11. (Color online) (a) Lyapunov exponents (solid red line in the upper portion and dashed blue line in the lower portion of the figure) and real part of the eigenvalues of the Jacobian (triangles and dots). (b) Common frequency (solid line) and the imaginary part of the eigenvalues of the Jacobian (triangles and dots).

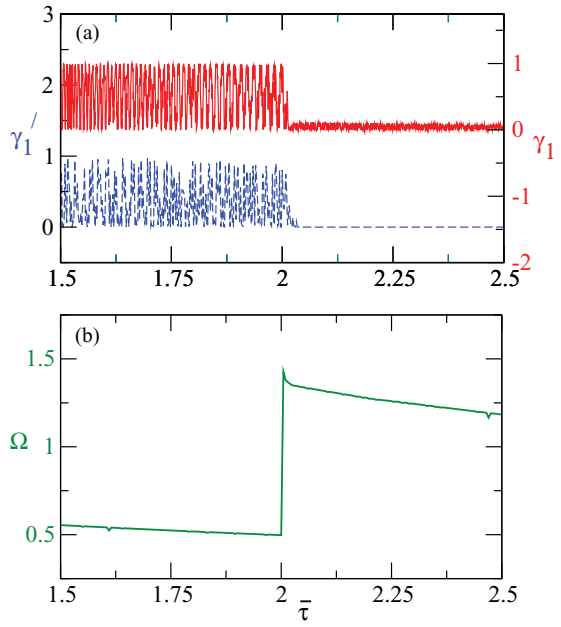

FIG. 12. (Color online) (a) Order parameter γ_1 showing the change in behavior of the eigenvectors at the delay value where transition occurs. The blue dashed curve in the lower portion of the figure corresponds to the case of symmetric delays in the coupling, whereas the solid red curve (upper portion) shows the behavior of the order parameter for the asymmetric case with $\tau_1 = 0$ and $\tau_2 = 2\tau$. (b) Frequency Ω for the system with asymmetric time delay in the coupling with $\tau_1 = 0$ and $\tau_2 = 2\tau$.

we obtain

$$c_1\beta + c_2(2\alpha\beta) + c_3(3\alpha^2\beta - \beta^3) + c_4(4\alpha^3\beta - 4\alpha\beta^3) + c_5(5\alpha^4\beta - 10\alpha^2\beta^3 + \beta^5) + c_6(6\alpha^5\beta + 6\alpha\beta^5 - 20\alpha^3\beta^3) - [b_0 + b_1\alpha + b_2(\alpha^2 - \beta^2) + b_3(\alpha^3 - 3\alpha\beta^2) + b_4(\alpha^4 + \beta^4 - 6\alpha^2\beta^2)]\sin(2\beta\bar{\tau})e^{-2\alpha\bar{\tau}} + [b_1\beta + b_2(2\alpha\beta) + b_3(3\alpha^2\beta - \beta^3) + b_4(4\alpha^3\beta - 4\alpha\beta^3)]\cos(2\beta\bar{\tau})e^{-2\alpha\bar{\tau}} = 0. \quad (29)$$

The real part α and the imaginary part β in the AD regime are plotted with Lyapunov exponents and frequencies, respectively (Fig. 11). In Fig. 11, we once again observe the "avoided crossing" of the Lyapunov exponents. Pairs of eigenvalues interchange imaginary parts at the crossing, as in the case of limit-cycle oscillators [21], resulting in frequency and phase jump. The variation of order parameter γ [Eq. (17)] for the Rössler case is shown in Fig. 12.

IV. SUMMARY

Phase flip has been observed in a wide variety of systems [20]. The universality of phase flip in systems coupled with identical delays makes this study on the mechanism of phase flip with asymmetric delays quite relevant.

In this work, we have analyzed the behavior of Landau-Stuart oscillators and Rössler oscillators coupled through asymmetric time delays. Although such systems also exhibit behavior similar to the symmetric delay case, the transition corresponds to a change in the relative phase that differs from π and depends on the difference in the coupling delays. Some characteristics of this transition are shared by an equivalent symmetric delay case: the Lyapunov spectrum and the frequency response of the system only depends on the average delay within the amplitude death regime. As noted earlier, there is an avoided crossing in the Lyapunov spectrum at the point where the relative phases change abruptly. The eigenvalue analysis shows that this corresponds to an exchange in the imaginary parts of the eigenvalues as for the symmetric case. There is sufficient evidence regarding the presence of similar phenomena and mechanisms for other coupled systems as well.

The simplification of a general chaotic system into its phase and amplitude parts can facilitate the analysis of the asymmetric delay-coupling case. However, the derivation of the dynamical equation for the phase of a chaotic oscillator is a nontrivial problem. In this paper we were able to exploit the phase coherence of the Rössler system for obtaining the estimates of the phase dynamics. The analysis of a general chaotic system where phase is not defined [29] still remains a challenging and open problem.

ACKNOWLEDGMENTS

The authors would like to acknowledge the anonymous reviewers for their constructive remarks and suggestions. R.K. acknowledges support from the University Grants Commission, India, and VolkswagenStiftung Germany. N.P., A.P., and R.R. acknowledge the Department of Science and Technology for research support. A.P. acknowledges the kind hospitality of the MPI-PKS Dresden, Germany.

[1] M. Lakshmanan and D. V. Senthilkumar, *Dynamics of Nonlinear Time-Delay Systems* (Springer-Verlag, Berlin, 2011).
[2] F. M. Atay, *Complex Time-Delay Systems* (Springer-Verlag, Berlin, 2010).
[3] H. G. Schuster and P. Wagner, Prog. Theor. Phys. **81**, 939 (1989).
[4] C. Huygens, *Horoloquium Oscilatorium* (Parisiis, Paris, 1673).
[5] K. Kaneko, *Theory and Applications of Coupled Map Lattices* (John Wiley and Sons, New York, 1993); L. M. Pecora and T. L. Carroll, Phys. Rev. Lett. **64**, 821 (1990); A. Prasad, L. D. Iasemidis, S. Sabesan and K. Tsakalis, Pramana, J. Phys. **64**, 513 (2005).
[6] A. Pikovsky, M. Rosenblum, and J. Kurths, *Synchronization, A Universal Concept in Nonlinear Science* (Cambridge University Press, Cambridge, England, 2001).
[7] M. Bennett, M. F. Schatz, H. Rockwood, and K. Wiesenfeld, Proc. R. Soc. London **458**, 563 (2002).
[8] Numerically, however, this limit is difficult to demonstrate.
[9] K. Bar-Eli, Physica D **14**, 242 (1985).

[10] D. V. Ramana Reddy, A. Sen, and G. L. Johnston, Phys. Rev. Lett. **80**, 5109 (1998).

[11] R. E. Mirollo and S. H. Strogatz, J. Stat. Phys. **60**, 245 (1990); G. B. Ermentrout, Physica D **41**, 219 (1990); S. H. Strogatz, Nature (London) **394**, 316 (1998); D. V. R. Reddy, A. Sen, and G. L. Johnston, Physica D **129**, 15 (1999).

[12] D. G. Aronson, G. B. Ermentrout, and N. Koppel, Physica D **41**, 403 (1990).

[13] A. Prasad, Phys. Rev. E **72**, 056204 (2005).

[14] R. Karnatak, R. Ramaswamy, and A. Prasad, Phys. Rev. E **76**, 035201(R) (2007).

[15] K. Konishi, Phys. Rev. E **68**, 067202 (2003).

[16] A. Prasad, M. Dhamala, B. M. Adhikari, and R. Ramaswamy, Phys. Rev. E **81**, 027201 (2010); **82**, 027201 (2010); A. Prasad, Chaos, Solitons Fractals **43**, 42 (2010).

[17] F. M. Atay, Phys. Rev. Lett. **91**, 094101 (2003).

[18] G. Saxena, A. Prasad, and R. Ramaswamy, Phys. Rev. E **82**, 017201 (2010).

[19] A. Prasad, J. Kurths, S. K. Dana, and R. Ramaswamy, Phys. Rev. E **74**, 035204(R) (2006).

[20] A. Prasad, S. K. Dana, R. Karnatak, J. Kurths, B. Blasius, and R. Ramaswamy, Chaos **18**, 023111 (2008).

[21] R. Karnatak, N. Punetha, A. Prasad, and R. Ramaswamy, Phys. Rev. E **82**, 046219 (2010).

[22] The models, Eqs. (3) and (18), are integrated using the Runge-Kutta fourth-order scheme with integration step $\Delta t = \tau/N$, where discreteness $N = 1000$ for the Landau-Stuart system and 2000 for the Rössler system. The random numbers in $[0,1]$ are used for initial conditions in the interval $[-\tau,0]$. Figures 1, 2, 7, and 8 are calculated in a 100×100 grid.

[23] V. Ahlers, R. Zillmer, and A. Pikovsky, Phys. Rev. E **63**, 036213 (2001).

[24] O. Rössler, Phys. Lett. A **57**, 397 (1976).

[25] The largest Lyapunov exponent of uncoupled Rössler systems for the given values of parameters is approximately around 0.08.

[26] M. G. Rosenblum, A. S. Pikovsky, and J. Kurths, Phys. Rev. Lett. **78**, 4193 (1997).

[27] The stable fix point $x_1^* = x_2^* = \frac{1}{2\omega}(c\omega - \sqrt{c^2\omega^2 - 4af}) = 0.003$; $y_1^* = y_2^* = -\frac{1}{2a}(c\omega - \sqrt{c^2\omega^2 - 4af}) = -0.020$ and $z_1^* = z_2^* = \frac{\omega}{2a}(c\omega - \sqrt{c^2\omega^2 - 4af}) = 0.020$.

[28] The characteristic equation for the Jacobian at the fixed point is $53.58 + 206.40\lambda + 364.65\lambda^2 + 334.14\lambda^3 + 156.60\lambda^4 + 22.66\lambda^5 + \lambda^6 - 6.12e^{-2\lambda\tau} + 72.97e^{-2\lambda\tau}\lambda - 210.06e^{-2\lambda\tau}\lambda^2 - 44.24e^{-2\lambda\tau}\lambda^3 - 2.25e^{-2\lambda\tau}\lambda^4 = 0$.

[29] In some systems, phases can only be defined by certain transformations. We also observed similar numerical results (results not included here) showing the agreement between different delay and equivalent delay frequencies and Lyapunov exponents for the Lorenz system: $\dot{x}_i = -\sigma(x_i - y_i)$; $\dot{y}_i = -x_i z_i - y_i + r x_i + \epsilon[y_j(t - \tau_i) - y_i]$; and $\dot{z}_i = x_i y_i - d z_i$; with $i, j = 1,2 (i \neq j)$ and the parameter values $\sigma = 10.0, r = 28.0, d = 8/3, \epsilon = 0.5$. Here the phase is defined as [6] $\phi = \arctan(\frac{z - z_0}{u - u_0})$, using the transformation $u(t) = \sqrt{(x^2 + y^2)}$, where u_0 and z_0 are fixed points.